

**Role insolation and greenhouse gases in timing peak warmth**

P. M. Langebroek and  
K. H. Nisancioglu

# Simulating last interglacial climate with NorESM: role of insolation and greenhouse gases in the timing of peak warmth

P. M. Langebroek<sup>1,2</sup> and K. H. Nisancioglu<sup>2,3</sup>

<sup>1</sup>Uni Climate, Uni Research, Allégaten 55, 5007 Bergen, Norway

<sup>2</sup>Bjerknes Centre for Climate Research, Allégaten 55, 5007 Bergen, Norway

<sup>3</sup>Department of Earth Science, University of Bergen, Allégaten 41, 5007 Bergen, Norway

Received: 15 July 2013 – Accepted: 17 July 2013 – Published: 7 August 2013

Correspondence to: P. M. Langebroek (petra.langebroek@uni.no)

Published by Copernicus Publications on behalf of the European Geosciences Union.

[Title Page](#)

[Abstract](#)

[Introduction](#)

[Conclusions](#)

[References](#)

[Tables](#)

[Figures](#)

[⏪](#)

[⏩](#)

[◀](#)

[▶](#)

[Back](#)

[Close](#)

[Full Screen / Esc](#)

[Printer-friendly Version](#)

[Interactive Discussion](#)

## Abstract

The last interglacial (LIG) is characterized by high latitude warming and is therefore often considered as a possible analogue for future warming. However, in contrast to predicted future greenhouse warming, the last interglacial climate is largely governed by variations in insolation. Greenhouse gas (GHG) concentrations were relatively stable and similar to pre-industrial values, with the exception of the early last interglacial where GHGs were slightly lower.

We performed six time-slice simulations with the low resolution version of the Norwegian Earth System Model covering the last interglacial. In four simulations only orbital forcing was changed, and in two simulations additionally GHG forcing was reduced to values appropriate for the early last interglacial.

Our simulations show that insolation forcing results in seasonal and hemispheric differences in temperature. In contrast, a reduction in greenhouse gas forcing causes a global and seasonal-independent cooling. We also compare our modelled results to proxy data extracted from four marine sediment cores covering the entire last interglacial along a northeast-southwest transect in the North Atlantic. Our modelled North Atlantic summer sea surface temperatures capture the general trend of the proxy summer temperatures, with low values in the early last interglacial, a peak around 125 ka, and a steady decrease towards the end of the last interglacial. Temperatures computed by the simulations with reduced GHG forcing improve the fit as they show lower temperatures in the early last interglacial. Furthermore we show that the timing of maximum surface temperatures follows the local insolation maximum. Two exceptions are the temperatures on Antarctica that show maxima at both  $\sim 130$  ka and  $\sim 115$  ka, and the Southern Ocean austral summer temperatures that peak early at  $\sim 130$  ka. This is probably due to the integrating effect of the ocean, storing summer heat and resulting in relatively warm winter temperatures.

## Role insolation and greenhouse gases in timing peak warmth

P. M. Langebroek and  
K. H. Nisancioglu

[Title Page](#)

[Abstract](#)

[Introduction](#)

[Conclusions](#)

[References](#)

[Tables](#)

[Figures](#)



[Back](#)

[Close](#)

[Full Screen / Esc](#)

[Printer-friendly Version](#)

[Interactive Discussion](#)



# 1 Introduction

The last interglacial period (LIG, ~ 130–116 ka, ka = 1000 yr ago) is often considered as an analogue for future climate warming (e.g. Kukla et al., 2002; Jansen et al., 2007; Clark and Huybers, 2009). Indeed, the early LIG is characterized by warm high latitude climates (e.g. CAPE Last Interglacial Project Members, 2006), and approximately 7 m higher sea level than today (Kopp et al., 2009). However, in contrast to the predicted future greenhouse warming, the climate of the last interglacial is governed by variations in solar insolation. Atmospheric CO<sub>2</sub> concentrations were close to, or slightly below pre-industrial values (280 ppm; Petit et al., 1999; Luëthi et al., 2008), as were the other main greenhouse gas (GHG) concentrations (Loulergue et al., 2008; Schilt et al., 2010).

In addition to numerous studies based on marine proxies (e.g. Leduc et al., 2010; Van Nieuwenhove et al., 2011), a few recent studies have compared reconstructed climate of the last interglacial to equilibrium simulations with general circulation models (GCMs) (e.g. Born et al., 2011; Govin et al., 2012; Lunt et al., 2013). To first order, the simulated and reconstructed interglacial mean surface ocean temperatures are comparable and show warm high latitudes, in particular in the North Atlantic. However, for the early part of the last interglacial marine proxies show colder conditions in the North Atlantic, Labrador and Norwegian Seas compared to model simulations. One possible reason for this is the input of freshwater to the North Atlantic from melting of the remnants of the Saalian ice sheets (penultimate glacial period) (Govin et al., 2012).

On land, Kaspar et al. (2005) compare atmospheric climate model results to paleobotanically derived European temperatures for 125 ka. They find a good match between reconstructed and simulated higher temperatures in the early last interglacial, and conclude that the different orbital parameters are sufficient to explain the reconstructed patterns over Europe. Lunt et al. (2013) compare last interglacial temperatures computed by an ensemble of equilibrium climate model simulations to a global temperature reconstruction (sea-surface and land temperatures) compiled by Turney and Jones

CPD

9, 4449–4473, 2013

## Role insolation and greenhouse gases in timing peak warmth

P. M. Langebroek and  
K. H. Nisancioglu

Title Page

Abstract

Introduction

Conclusions

References

Tables

Figures

⏪

⏩

◀

▶

Back

Close

Full Screen / Esc

Printer-friendly Version

Interactive Discussion

## Role insolation and greenhouse gases in timing peak warmth

P. M. Langebroek and  
K. H. Nisancioglu

Title Page

Abstract

Introduction

Conclusions

References

Tables

Figures

⏪

⏩

◀

▶

Back

Close

Full Screen / Esc

Printer-friendly Version

Interactive Discussion

(2010). They show that the modelled annual mean surface air temperatures over land do not correspond well with the reconstructed LIG temperatures. Comparing simulated summer surface air temperatures to the proxy dataset, instead of annual mean, improves the fit, although large discrepancies still exist. Lunt et al. (2013) also find that their simulated ensemble mean annual sea surface temperature underestimates North Atlantic sea surface temperatures for the last interglacial when compared with the marine proxies.

We will go one step further than previous studies by comparing seasonal output from four time-slice simulations to four high-resolution proxy records from the North Atlantic. These records have a relatively high resolution and are all transferred to one common time scale, so no additional errors will be induced when comparing the records to each other. We focus on the North Atlantic/Nordic Seas because these regions are particularly sensitive to changes in climate forcing and are thought to endure large environmental changes in the near future (e.g. Meehl et al., 2007; Lenton et al., 2008).

Before we discuss the comparison between our simulated temperatures and the last interglacial proxy records, we will assess the relative effects of greenhouse gas and solar insolation forcing on the simulated last interglacial climate. Finally we will evaluate the timing of peak last interglacial warmth in our simulations, and document its strong dependence on latitude and whether the locality is over ocean or land.

## 2 Methods and experimental set-up

### 2.1 The Norwegian Earth System Model

The Norwegian Earth System Model (NorESM) is derived from the Community Earth System Model (CESM) developed at the National Center for Atmospheric Research (NCAR). It consists of the same components for the atmosphere (CAM4), land (CLM4) and sea ice (CICE4), and uses the CESM coupler (CLP7). However, a key difference with CESM is the use of a different ocean component, based on the Miami Isopycnic

## Role insolation and greenhouse gases in timing peak warmth

P. M. Langebroek and  
K. H. Nisancioglu

[Title Page](#)[Abstract](#)[Introduction](#)[Conclusions](#)[References](#)[Tables](#)[Figures](#)[⏪](#)[⏩](#)[◀](#)[▶](#)[Back](#)[Close](#)[Full Screen / Esc](#)[Printer-friendly Version](#)[Interactive Discussion](#)

Coordinate Ocean Model (MICOM). This component is largely modified from MICOM in order to improve conservation of mass and heat, and the efficiency and robustness of the transport of tracers (for more details see Assmann et al., 2010). Furthermore the NorESM CAM model (CAM-Oslo) optionally provides a detailed treatment of atmospheric chemistry, aerosols and clouds (Seland et al., 2008).

NorESM participates in the fifth phase of the Climate Model Intercomparison Project (CMIP5; e.g. Taylor et al., 2012). For an in-depth description of NorESM and its climate response to CMIP scenarios we refer to Bentsen et al. (2013) and Iversen et al. (2013), respectively.

The simulations in this study are performed with the low-resolution version of NorESM (NorESM-L) in order to reduce computation time and allow for several equilibrium simulations. The atmospheric component has a spatial resolution of approximately  $3.75^\circ \times 3.75^\circ$  (T31) and comprises of 26 levels in the vertical. The ocean component's horizontal grid size corresponds to a nominal grid size of  $3^\circ$  (g37) and consists of 30 isopycnic layers in the vertical. The sea-ice component follows the ocean grid, and the land component follows the atmospheric grid. For further details concerning the different components within NorESM-L we refer to Zhang et al. (2012). This paper also describes the results from the pre-industrial and mid-Pliocene simulations. Additional experiments for warmer (last millennium and 6 ka) and colder (Last Glacial Maximum) then present paleo time slices are currently being performed with NorESM-L. These all follow the set-up as defined by the Paleoclimate Modelling Intercomparison Project 3 (PMIP3).

## 2.2 Experimental set-up

We performed seven time-slice simulations with NorESM-L: one pre-industrial (PI) control experiment and six last interglacial (LIG) simulations (see Table 1). All simulations use the modern land-sea distribution, topography, ice sheets and vegetation, as constituted in CESM (Versteinsten et al., 2012), as well as modern ocean bathymetry.

## Role insolation and greenhouse gases in timing peak warmth

P. M. Langebroek and  
K. H. Nisancioglu

[Title Page](#)[Abstract](#)[Introduction](#)[Conclusions](#)[References](#)[Tables](#)[Figures](#)[⏪](#)[⏩](#)[◀](#)[▶](#)[Back](#)[Close](#)[Full Screen / Esc](#)[Printer-friendly Version](#)[Interactive Discussion](#)

In the PI simulation atmospheric greenhouse gas concentrations are set to pre-industrial values of CO<sub>2</sub>, CH<sub>4</sub> and N<sub>2</sub>O (see Table 1) and zero levels of chlorofluorocarbons (CFCs). Orbital parameters are set to values for the year 1950 (Berger, 1978). The ocean model is initialized from modern observed temperatures and salinities (Levitus and Boyer, 1994). While keeping the orbital configuration and greenhouse gases fixed, the PI control simulation is run for 1500 yr.

The LIG simulations are branched off from the PI simulation at model year 495, when the PI run is close to equilibrium. Four LIG time-slice simulations are performed with fixed pre-industrial greenhouse gases, but with orbital parameters of 115 ka, 120 ka, 125 ka and 130 ka. These experiments are given the suffix G<sub>pi</sub> in Table 1 denoting Greenhouse gas levels (G) at pre-industrial (pi) levels. Two LIG simulations (125 ka\_G<sub>pi</sub> and 130 ka\_G<sub>pi</sub>) are repeated using the lower greenhouse gas levels as set by PMIP based on Petit et al. (1999); Luëthi et al. (2008); Louergue et al. (2008) and Schilt et al. (2010) (see 125 ka and 130 ka in Table 1). All LIG simulations are run another 505 yr (from model year 495 to 1000) using the new orbital and greenhouse gas forcing.

All simulations are close to equilibrium in model year 900. The model results presented in this study are therefore based on the years 901 to 1000 of each simulation. The global mean ocean temperature trend during this final period is found to be small at 0.006–0.024 °C/100 yr.

### 2.3 Sediment data used for model-data comparison

We compare our last interglacial model results to proxy data extracted from four marine sediment cores along a northeast-southwest transect in the North Atlantic (Table 2). These cores cover the entire period of interest (115–130 ka) and have a relatively high sedimentation rate (~ 5 to 17 cm yr<sup>-1</sup>). Govin et al. (2012) transferred these sediment cores to one single time scale based on the Greenland NGRIP δ<sup>18</sup>O ice core record (North Greenland Ice Core Project members, 2004). The total age uncertainty of less than 2500 yr combines uncertainties in the resolution of the records and the procedure transferring all records to a common time scale (Govin et al., 2012).

We compare our model results to the reconstructed summer sea-surface temperatures (SST) as provided by Govin et al. (2012), where the SSTs of MD95-2010 and EW9302-JPC2 are reconstructed using the percentage of the polar species *Neoglobobulimina pachyderma* sinistral, and the SSTs of ODP 980 and CH69-K09 are reconstructed using the Modern Analogue Technique on planktonic foraminifera faunal assemblages. Other proxies (e.g. ice rafted debris, stable isotopes) are not considered in this study. For a detailed discussion of the sediment core data and dating procedure, we refer to Govin et al. (2012) and the original references in Table 2.

### 3 Results and discussion

#### 3.1 Simulated seasonal and hemispheric surface air temperatures

We performed four simulations every 5000 yr covering the last interglacial by only changing the orbital forcing (115 ka\_Gpi, 120 ka\_Gpi, 125 ka\_Gpi and 130 ka\_Gpi). Although the global annual mean incoming insolation is similar for all four runs (Fig. 1a), their latitudinal and seasonal distribution is significantly different (Fig. 1b–e).

The early last interglacial (130 ka and 125 ka) shows enhanced Northern Hemisphere spring/summer insolation compared to pre-industrial conditions. Accompanied with reduced Northern Hemisphere autumn/winter insolation this gives a stronger seasonal cycle in the early part of the last interglacial. The opposite occurs in the late last interglacial (115 ka), where a relatively cold Northern Hemisphere spring/summer is combined with a warm autumn/winter, reducing the seasonal insolation contrast. In the Southern Hemisphere (SH) the early last interglacial summer/autumn insolation is enhanced, while winter insolation is reduced. Spring insolation is fairly similar to today. The combined effect is a slightly weaker seasonal cycle in the Southern Hemisphere in the early part of the last interglacial. The late last interglacial (115 ka) Southern Hemisphere seasonal insolation cycle is strengthened due to relatively warm austral summers (especially at low latitudes) and slightly colder austral winters (Fig. 1d and e).

## Role insolation and greenhouse gases in timing peak warmth

P. M. Langebroek and  
K. H. Nisancioglu

Title Page

Abstract

Introduction

Conclusions

References

Tables

Figures



Back

Close

Full Screen / Esc

Printer-friendly Version

Interactive Discussion



## Role insolation and greenhouse gases in timing peak warmth

P. M. Langebroek and  
K. H. Nisancioglu

[Title Page](#)[Abstract](#)[Introduction](#)[Conclusions](#)[References](#)[Tables](#)[Figures](#)[Back](#)[Close](#)[Full Screen / Esc](#)[Printer-friendly Version](#)[Interactive Discussion](#)

The simulated global mean surface air temperature follows the Northern Hemisphere insolation pattern, with a strong seasonal cycle in the early LIG experiments (130 ka\_Gpi and 125 ka\_Gpi) and reduced seasonal contrasts in the late LIG (120 ka\_Gpi and 115 ka\_Gpi). This pattern is most pronounced when considering Northern Hemisphere seasonal mean temperatures (Fig. 2a), while the Southern Hemisphere temperatures show the opposite trend (Fig. 2b).

The two early LIG simulations with reduced greenhouse gas forcing (130 ka and 125 ka) give the same seasonal contrast in hemispheric mean surface air temperatures (not shown), albeit with slightly smaller absolute values.

Figure 3 illustrates the difference between orbital and greenhouse gas forcing for the two 130 ka simulations (130 ka and 130 ka\_Gpi), which have the largest difference in greenhouse gas forcing (23 ppm; Table 1). The reduced greenhouse gas forcing results in a temperature reduction similar in all seasons and both hemispheres (Fig. 3 right column). In contrast the 130 ka insolation changes cause seasonal and hemispheric differences in surface air temperature. The relatively large annual mean warming found in high latitudes (mainly southern high latitudes), compared to the relatively small change in annual mean insolation, is mainly due to the strong summer sea ice melting.

### 3.2 North Atlantic sea-surface temperatures

The evolution of summer SSTs measured in the four North Atlantic sediment cores through the last interglacial (Table 2) is shown together with simulated temperatures in Fig. 4. The temperature data from ODP 980 and CH69-K09 have a higher resolution and are therefore 3-point smoothed (as is also done in Govin et al., 2012). The three northern most cores (MD95-2010, ODP 980 and EW9302-JPC02) all show an increase in SSTs early in the last interglacial, with maximum temperatures around 125 ka, and a decrease towards 115 ka. In contrast, the southernmost core in the North Atlantic (CH69-K09) records a steady increase from 130 ka, reaching a maximum at ~ 119 ka, with only a very minor decrease thereafter.



## Role insolation and greenhouse gases in timing peak warmth

P. M. Langebroek and  
K. H. Nisancioglu

[Title Page](#)[Abstract](#)[Introduction](#)[Conclusions](#)[References](#)[Tables](#)[Figures](#)[Back](#)[Close](#)[Full Screen / Esc](#)[Printer-friendly Version](#)[Interactive Discussion](#)

We compare the sediment core data to our LIG simulations (Fig. 4) by extracting mean monthly SSTs (representing the upper  $\sim 10$  m of the water column) from the ocean grid boxes surrounding the sediment core locations. The dashed lines represent the LIG evolution based on the four simulations using pre-industrial greenhouse gases.

The simulated summer (July, August and September) temperatures follow the general pattern of the sediment core data. For the early part of the period this fit to the proxy data is improved when including reduced GHG concentrations (experiments 130 ka and 125 ka; dotted lines in Fig. 4).

The results presented here are computed from time-slice simulations, not from a transient simulation. However, we expect a smooth transition from one time-slice experiment to the next, as the orbital and GHG forcing changes slowly over this period. In case dynamic ice sheets are included, the climate response may be more abrupt and a transient simulation would be necessary.

In order to explain the reconstructed low temperatures of the early last interglacial, Govin et al. (2012) suggest that (in addition to the altered orbital configuration) there was inflow of meltwater to the North Atlantic from remnants of the glacial ice sheets. Our simulations show evidence of significantly lower surface ocean temperatures solely by reducing the levels of atmospheric greenhouse gases, without including freshwater from melting ice sheets. Both, freshwater inflow and reduced GHG concentrations, together or separately could help explain the relatively cold temperatures at the start of the last interglacial.

Even though the general temperature evolution during the last interglacial is captured by the simulations, the model underestimates the temperatures at the two northernmost core locations by  $\sim 2\text{--}3^\circ\text{C}$  (MD95-2010 and ODP 980; Fig. 4a, b). This might be due to reduced inflow of relatively warm Atlantic water into the Nordic Seas, causing too cold modelled temperatures at the northern most cores. On the other hand, also the reconstructed SSTs can be too high. The Norwegian Sea (core MD95-2010) SST estimates are derived from a defined linear relationship between the percentage of a polar foraminifera species (*N. pachyderma* sinistral) and summer SSTs from the

## Role insolation and greenhouse gases in timing peak warmth

P. M. Langebroek and  
K. H. Nisancioglu

Title Page

Abstract

Introduction

Conclusions

References

Tables

Figures

⏪

⏩

◀

▶

Back

Close

Full Screen / Esc

Printer-friendly Version

Interactive Discussion

MARGO dataset. The total error on this calibration is 1.8 °C (Govin et al., 2012). The SSTs at the North Atlantic core ODP 980 are reconstructed using the Modern Analogue Technique on foraminifera faunal assemblages. The error bar for this temperature reconstruction is between 0.5 and 2 °C (Cortijo et al., 1999). Hence within the model and data uncertainties the records fit well to the modelled temperatures.

Another probable source for the mismatch between modelled and reconstructed SSTs relates to the depth at which the foraminifera live and create the shell that captures the ocean conditions. This habitat depth differs from species to species, and could easily be below the upper 10 m of the water column, the value defining sea surface in NorESM. However, as the reconstructed temperatures are calibrated to ocean temperatures taken at 10 m water depth, errors occurring will be small compared to the standard calibration error (see above).

The reconstructed maximum summer SSTs at ~ 125 ka, as depicted by the three northernmost sediment cores, is a large-scale phenomenon also simulated by the model for the North Atlantic (Fig. 5). The warmth is most pronounced at the continental margins, and is not captured by the open ocean sediment core locations. In contrast to the general pattern of warming, the SSTs in the centre of the North Atlantic are colder during the last interglacial, a feature most pronounced during the early warm last interglacial (125 ka and 130 ka). This is due to a slightly expanded subpolar gyre (not shown) early in the last interglacial, shifting the separation between relatively cold subpolar water and warm subtropical water further southeast.

### 3.3 Timing of maximum last interglacial warmth

Recent studies discuss the timing of the maximum warmth during the last interglacial (e.g. Govin et al., 2012; Bakker et al., 2013). SST data from the Southern Ocean indicate an early maximum, possibly preceding the temperature increase in the Northern Hemisphere (Govin et al., 2012). In contrast, transient model simulations covering this time period show SH January peak warmth only after ~ 120 ka (Bakker et al., 2013).

## Role insolation and greenhouse gases in timing peak warmth

P. M. Langebroek and  
K. H. Nisancioglu

[Title Page](#)

[Abstract](#)

[Introduction](#)

[Conclusions](#)

[References](#)

[Tables](#)

[Figures](#)



[Back](#)

[Close](#)

[Full Screen / Esc](#)

[Printer-friendly Version](#)

[Interactive Discussion](#)

Figure 6 shows the timing of maximum insolation (Fig. 6a and b) and peak warmth (Fig. 6c–f) for our LIG simulations (reduced GHG simulations not shown). We show longitudinal mean values, as the variations in this direction are small compared to the latitudinal and seasonal differences. The values are normalized per latitude so that the peak warmth per latitude can easily be recognized. For further clarity we exclude results for latitudes where the insolation varies less than  $5 \text{ W m}^{-2}$  (Fig. 6a, b) and where the temperature varies less than half of the mean variations ( $0.7^\circ\text{C}$  for Fig. 6c, d and  $0.3^\circ\text{C}$  for Fig. 6e, f).

Summer (JJA) insolation is at its maximum at 125 ka for most latitudes. Only at high SH latitudes, 125 ka and 130 ka show a combined maximum. Winter (DJF) insolation has a late LIG (115 ka) maximum, with an exception for the Arctic Ocean, which has a slightly earlier maximum (120 ka).

The NH temperatures largely follow local insolation, with early peak warmth in summer ( $\sim 130$ – $125$  ka) and a late peak warmth in winter ( $\sim 120$ – $115$  ka). SH temperatures also largely follow the insolation pattern, until the mid to high southern latitudes. Between  $\sim 45^\circ\text{S}$  and  $90^\circ\text{S}$  in both winter and summer, above land and ocean, the temperature peaks at around 130 ka. Above Antarctica 115 ka also shows high austral summer (DJF) temperatures, and therefore the Antarctic summer peak warmth could either occur late or early in the last interglacial. This is in contrast with the clear early summer peak warmth in the Southern Ocean, and hence explains both the early Southern Ocean peak as found by Govin et al. (2012) and the late Antarctica peak described by Bakker et al. (2013).

The fact that the Southern Ocean peaks early also in austral summer, while direct insolation is still relatively low shows the integrating effect of the ocean: at high latitudes of the Southern Hemisphere (above  $\sim 40^\circ\text{S}$ ), which is dominated by ocean, summer insolation is efficiently stored and results in warm surface temperatures also in winter. This occurs not only over the ocean, but less effectively also over adjacent land surfaces (Antarctica).

## Role insolation and greenhouse gases in timing peak warmth

P. M. Langebroek and  
K. H. Nisancioglu

[Title Page](#)[Abstract](#)[Introduction](#)[Conclusions](#)[References](#)[Tables](#)[Figures](#)[Back](#)[Close](#)[Full Screen / Esc](#)[Printer-friendly Version](#)[Interactive Discussion](#)

Reducing the GHG concentrations in the early last interglacial (125 and 130 ka) results in a similar timing of peak warmth (not shown), except over Antarctica. There, the lower GHG reduce the early last interglacial temperatures. As a consequence the peak warmth shifts to 115 ka, even more confirming the results of Bakker et al. (2013).

### 4 Conclusions

We performed six time-slice simulations with the low resolution version of the Norwegian Earth System Model (NorESM1-L) covering the last interglacial (LIG) from 130 to 115 ka. In four simulations only orbital forcing was changed representing 130, 125, 120 and 115 ka. The two early LIG (130 and 125 ka) simulations were repeated with reduced greenhouse gas (GHG) forcing.

Our simulations show small changes in annual mean atmospheric temperatures, but a significant change in seasonal temperatures over the last interglacial. In the Northern Hemisphere the seasonal cycle is enhanced early in the last interglacial, and reduced in the later part. The Southern Hemisphere temperatures indicate the opposite, with a smaller seasonal contrast early in the last interglacial and a similar or slightly larger seasonal cycle later. We show that the seasonal and hemispheric differences are the result of insolation forcing. In contrast, a reduction in greenhouse gas forcing causes a global and seasonal-independent cooling.

The NorESM1-L simulations capture the general trend of last interglacial summer SSTs, as shown by four sediment cores in the North Atlantic, confirming that the proxy temperatures represent summer. Including reduced greenhouse gas levels during the early part of the last interglacial period, as given by ice core data (e.g. Petit et al., 1999), improves the fit to the SST reconstructions showing colder temperatures. Although the fit to the proxy data is improved by lower GHG forcing, we cannot exclude the possible influence of enhanced freshwater input from melting glaciers and ice sheets (as proposed by Govin et al., 2012) when explaining the reconstructed cold surface ocean temperatures of the North Atlantic in the early last interglacial.

## Role insolation and greenhouse gases in timing peak warmth

P. M. Langebroek and  
K. H. Nisancioglu

Title Page

Abstract

Introduction

Conclusions

References

Tables

Figures

⏪

⏩

◀

▶

Back

Close

Full Screen / Esc

Printer-friendly Version

Interactive Discussion

In general, the timing of peak warmth follows the local insolation maximum, with two main exceptions. First, the Southern Oceans austral summer peak warmth occurs already in the early last interglacial ( $\sim 130$  ka), even though local insolation is only slightly increased. This is probably due to the integrating effect of the ocean, storing summer heat resulting in relatively warm winter temperatures. Second, Antarctica has two maxima in austral temperatures, around 130 and 115 ka. Here the early peak ( $\sim 130$  ka) could be the result of the adjacent warm Southern Ocean combined with intermediate insolation. Reduced GHG concentrations at the early last interglacial lower the Antarctic temperatures and cause a single late last interglacial peak warmth at  $\sim 115$  ka.

*Acknowledgements.* We thank Aline Govin for providing the sediment core temperatures and discussing an early comparison of this data to our model results. This project was funded by Past4Future “Climate change – Learning from the past climate”, a Collaborative Project under the 7th Framework Programme of the European Commission (grant agreement no. 243908). This is publication no. XXX from the Bjerknes Centre for Climate Research.

## References

- Assmann, K. M., Bentsen, M., Segschneider, J., and Heinze, C.: An isopycnic ocean carbon cycle model, *Geosci. Model Dev.*, 3, 143–167, doi:10.5194/gmd-3-143-2010, 2010. 4453
- Bakker, P., Stone, E. J., Charbit, S., Gröger, M., Krebs-Kanzow, U., Ritz, S. P., Varma, V., Khon, V., Lunt, D. J., Mikolajewicz, U., Prange, M., Renssen, H., Schneider, B., and Schulz, M.: Last interglacial temperature evolution – a model inter-comparison, *Clim. Past*, 9, 605–619, doi:10.5194/cp-9-605-2013, 2013. 4458, 4459, 4460
- Bentsen, M., Bethke, I., Debernard, J. B., Iversen, T., Kirkevåg, A., Seland, Ø., Drange, H., Roelandt, C., Seierstad, I. A., Hoose, C., and Kristjánsson, J. E.: The Norwegian Earth System Model, NorESM1-M – Part 1: Description and basic evaluation of the physical climate, *Geosci. Model Dev.*, 6, 687–720, doi:10.5194/gmd-6-687-2013, 2013. 4453
- Berger, A. L.: Long term variations of caloric insolation resulting from the Earth’s orbital elements, *Quaternary Res.*, 9, 139–167, 1978. 4454
- Born, A., Kageyama, M., and Nisancioglu, K. H.: Warm Nordic Seas delayed glacial inception in Scandinavia, *Clim. Past*, 6, 817–826, doi:10.5194/cp-6-817-2010, 2010.

**Role insolation and greenhouse gases in timing peak warmth**P. M. Langebroek and  
K. H. Nisancioglu[Title Page](#)[Abstract](#)[Introduction](#)[Conclusions](#)[References](#)[Tables](#)[Figures](#)[⏪](#)[⏩](#)[◀](#)[▶](#)[Back](#)[Close](#)[Full Screen / Esc](#)[Printer-friendly Version](#)[Interactive Discussion](#)

Born, A., Nisancioglu, K. H., and Risebrobakken, B.: Late Eemian warming in the Nordic Seas as seen in proxy data and climate models, *Paleoceanography*, 26, PA2207, doi:10.1029/2010PA002027, 2011. 4451

CAPE Last Interglacial Project Members: Last Interglacial Arctic warmth confirms polar amplification of climate change, *Quaternary Sci. Rev.*, 25, 1383–1400, 2006. 4451

Clark, P. U. and Huybers, P.: Interglacial and future sea level, *Nature*, 462, 856–857, 2009. 4451

Cortijo, E., Lehman, S., Keigwin, L., Chapman, M., Paillard, D., and Labeyrie, L.: Changes in meridional temperature and salinity gradients in the North Atlantic Ocean (30–72° N) during the last interglacial period, *Paleoceanography*, 14, 23–33, 1999. 4458, 4467

Govin, A., Braconnot, P., Capron, E., Cortijo, E., Duplessy, J.-C., Jansen, E., Labeyrie, L., Landais, A., Marti, O., Michel, E., Mosquet, E., Risebrobakken, B., Swingedouw, D., and Waelbroeck, C.: Persistent influence of ice sheet melting on high northern latitude climate during the early Last Interglacial, *Clim. Past*, 8, 483–507, doi:10.5194/cp-8-483-2012, 2012. 4451, 4454, 4455, 4456, 4457, 4458, 4459, 4460

Iversen, T., Bentsen, M., Bethke, I., Debernard, J. B., Kirkevåg, A., Seland, Ø., Drange, H., Kristjansson, J. E., Medhaug, I., Sand, M., and Seierstad, I. A.: The Norwegian Earth System Model, NorESM1-M – Part 2: Climate response and scenario projections, *Geosci. Model Dev.*, 6, 389–415, doi:10.5194/gmd-6-389-2013, 2013. 4453

Jansen, E., Overpeck, J. T., Briffa, K. R., Duplessy, J.-C., Joos, F., Masson-Delmotte, V., Olago, D., Otto-Bliesner, B., Peltier, W. R., Rahmstorf, S., Ramesh, R., Raynaud, D., Rind, D., Solomina, O., Villalba, R., and Zhang, D.: Palaeoclimate, in: *Climate Change 2007: The Physical Science Basis*, Contribution of Working Group I to the Fourth Assessment Report of the Intergovernmental Panel on Climate Change, edited by: Solomon, S., Qin, D., Manning, M., Chen, Z., Marquis, M., Averyt, K. B., Tignor, M., and Miller, H. L., Cambridge University Press, Cambridge, UK and New York, NY, USA, 2007. 4451

Kaspar, F., Köhl, N., Cubasch, U., and Litt, T.: A model-data comparison of European temperatures in the Eemian interglacial, *Geophys. Res. Lett.*, 32, L11703, doi:10.1029/2005GL022456, 2005. 4451

Kopp, R. E., Simons, F. J., Mitrovica, J. X., Maloof, A. C., and Oppenheimer, M.: Probabilistic assessment of sea level during the last interglacial stage, *Nature*, 462, 863–867, 2009. 4451

Kukla, G. J., Bender, M. L., de Beaulieu, J.-L., Bond, G., Broecker, W. S., Cleveringa, P., Gavin, J. E., Herbert, T. D., Imbrie, J., Jouzel, J., Keigwin, L. D., Knudsen, K.-L., Mc-

## Role insolation and greenhouse gases in timing peak warmth

P. M. Langebroek and  
K. H. Nisancioglu

Title Page

Abstract

Introduction

Conclusions

References

Tables

Figures

⏪

⏩

◀

▶

Back

Close

Full Screen / Esc

Printer-friendly Version

Interactive Discussion

Manus, J. F., Merkt, J., Muhs, D. R., Müller, H., Poore, R. Z., Porter, S. C., Seret, G., Shackleton, N. J., Turner, C., Tzedakis, P. C., and Winograd, I. J.: Last interglacial climates, *Quaternary Res.*, 58, 2–13, 2002. 4451

5 Labeyrie, L., Leclaire, H., Waelbroeck, C., Cortijo, E., Duplessy, J. C., Vidal, L., Elliot, M., and Le Coat, B.: Temporal variability of the surface and deep waters of the North West Atlantic Ocean at orbital and millennial scales, *Geophys. Monogr.*, 112, 77–98, 1999. 4467

Leduc, G., Schneider, R., Kim, J.-H., and Lohmann, G.: Holocene and Eemian sea surface temperature trends as revealed by alkenone and Mg/Ca paleothermometry, *Quaternary Sci. Rev.*, 29, 989–1004, 2010. 4451

10 Lenton, T. M., Held, H., Kriegler, E., Hall, J. W., Lucht, W., Rahmstorf, S., and Schellnhuber, H. J.: Tipping elements in the Earth's climate system, *P. Natl. Acad. Sci. USA*, 105, 1786–1793, 2008. 4452

Levitus, S. and Boyer, T. P.: *World Ocean Atlas Volume 4: Temperature*, NOAA Atlas NESDIS 4, US Government Printing Office, Washington, DC, 117 pp., 1994. 4454

15 Loulergue, L., Schilt, A., Spahni, R., Masson-Delmotte, V., Blunier, T., Lemieux, B., Barnola, J.-M., Raynaud, D., Stocker, T. F., and Chappellaz, J.: Orbital and millennial-scale features of atmospheric CH<sub>4</sub> over the past 800,000 years, *Nature*, 453, 383–386, 2008. 4451, 4454

20 Luëthi, D., Le Floch, M., Bereiter, B., Blunier, T., Barnola, J.-M., Siegenthaler, U., Raynaud, D., Jouzel, J., Fischer, H., Kawamura, K., and Stocker, T. F.: High-resolution carbon dioxide concentration record 650,000–800,000 years before present, *Nature*, 453, 379–382, 2008. 4451, 4454

Lunt, D. J., Abe-Ouchi, A., Bakker, P., Berger, A., Braconnot, P., Charbit, S., Fischer, N., Herold, N., Jungclaus, J. H., Khon, V. C., Krebs-Kanzow, U., Langebroek, P. M., Lohmann, G., Nisancioglu, K. H., Otto-Bliesner, B. L., Park, W., Pfeiffer, M., Phipps, S. J., Prange, M., Rachmayani, R., Renssen, H., Rosenbloom, N., Schneider, B., Stone, E. J., Takahashi, K., Wei, W., Yin, Q., and Zhang, Z. S.: A multi-model assessment of last interglacial temperatures, *Clim. Past*, 9, 699–717, doi:10.5194/cp-9-699-2013, 2013. 4451, 4452

25 McManus, J. F., Oppo, D. W., and Cullen, J.: A 0.5-million-year record of millennial-scale climate variability in the North Atlantic, *Science*, 283, 971–975, 1999. 4467

30 Meehl, G., Stocker, T. F., Collins, W. D., Friedlingstein, P., Gaye, A. T., Gregory, J. M., Kitoh, A., Knutti, R., Murphy, J. M., Noda, A., Raper, S. C. B., Watterson, I. G., Weaver, A. J., and Zhao, Z.-C.: Global climate projections, in: *Climate Change 2007: The Physical Science Basis*, Contribution of Working Group I to the Fourth Assessment Report of the Intergovern-

## CPD

9, 4449–4473, 2013

**Role insolation and greenhouse gases in timing peak warmth**P. M. Langebroek and  
K. H. Nisancioglu[Title Page](#)[Abstract](#)[Introduction](#)[Conclusions](#)[References](#)[Tables](#)[Figures](#)[⏪](#)[⏩](#)[◀](#)[▶](#)[Back](#)[Close](#)[Full Screen / Esc](#)[Printer-friendly Version](#)[Interactive Discussion](#)

mental Panel on Climate Change, edited by: Solomon, S., Qin, D., Manning, M., Chen, Z., Marquis, M., Averyt, K. B., Tignor, M., and Miller, H. L., Cambridge University Press, Cambridge, UK, and New York, NY, USA, 2007. 4452

North Greenland Ice Core Project members: High-resolution climate record of Northern Hemisphere climate extending into the last interglacial period, *Nature*, 431, 147–151, 2004. 4454

Oppo, D. W., McManus, J. F., and Cullen, J. L.: Evolution and demise of the Last Interglacial warmth in the subpolar North Atlantic, *Quaternary Sci. Rev.*, 25, 3268–3277, 2006. 4467

Petit, J., Jouzel, J., Raynaud, D., Barkov, N., Barnola, J.-M., Basile, I., Bender, M., Chappellaz, J., Davis, M., Delaygue, G., Delmotte, M., Kotlyakov, V., Legrand, M., Lipenkov, V., Lorius, C., Pépin, L., Ritz, C., Saltzman, E., and Stievenard, M.: Climate and atmospheric history of the past 420,000 years from the Vostok ice core, *Nature*, 399, 429–436, 1999. 4451, 4454, 4460

Rasmussen, T. L., Thomsen, E., Kuijpers, A., and Wastegård, S.: Late warming and early cooling of the sea surface in the Nordic seas during MIS 5e (Eemian Interglacial), *Quaternary Sci. Rev.*, 22, 809–821, 2003. 4467

Risebrobakken, B., Dokken, T., and Jansen, E.: Extent and variability of the Meridional Atlantic Circulation in the Eastern Nordic Seas during Marine Isotope Stage 5 and its influence on the inception of the last glacial, in: *The Nordic Seas: an Integrated Perspective*, edited by: Drange, H., Dokken, T., Furevik, T., Gerdes, R., and Berger, W. H., *Climate Variability in the Nordic Seas*, AGU Monograph, 20, 2005. 4467

Risebrobakken, B., Balbon, E., Dokken, T., Jansen, E., Kissel, C., Labeyrie, L., Richter, T., and Senneset, L.: The penultimate deglaciation: high-resolution paleoceanographic evidence from a north-south transect along the eastern Nordic Seas, *Earth Planet. Sc. Lett.*, 241, 505–516, 2006. 4467

Schilt, A., Baumgartner, M., Blunier, T., Schwander, J., Spahni, R., Fischer, H., and Stocker, T. F.: Glacial-interglacial and millennial-scale variations in the atmospheric nitrous oxide concentration during the last 800,000 years, *Quaternary Sci. Rev.*, 29, 182–192, 2010. 4451, 4454

Seland, Ø., Iversen, T., Kirkevåg, A., and Storelvmo, T.: Aerosol-climate interactions in the CAM-Oslo atmospheric GCM and investigation of associated basic shortcomings, *Tellus A*, 60, 459–491, 2008. 4453

Taylor, K. E., Stouffer, R. J., and Meehl, G. A.: An overview of CMIP5 and the experiment design, *B. Am. Meteorol. Soc.*, 93, 485–498, 2012. 4453





## Role insolation and greenhouse gases in timing peak warmth

P. M. Langebroek and  
K. H. Nisancioglu

Title Page

Abstract

Introduction

Conclusions

References

Tables

Figures

⏪

⏩

◀

▶

Back

Close

Full Screen / Esc

Printer-friendly Version

Interactive Discussion



Turney, C. S. and Jones, R. T.: Does the Agulhas Current amplify global temperatures during super-interglacials?, *J. Quaternary Sci.*, 25, 839–843, 2010. 4451

Van Nieuwenhove, N., Bauch, H. A., Eynaud, F., Kandiano, E., Cortijo, E., and Turon, J.-L.: Evidence for delayed poleward expansion of North Atlantic surface waters during the last interglacial (MIS 5e), *Quaternary Sci. Rev.*, 30, 934–946, 2011. 4451

Vertenstein, M., Craig, T., Middleton, A., Feddema, D., and Fischer, C.: CESM1.0.4 User's Guide, available at: [http://www.cesm.ucar.edu/models/cesm1.0/cesm/cesm\\_doc\\_1\\_0\\_4/book1.html](http://www.cesm.ucar.edu/models/cesm1.0/cesm/cesm_doc_1_0_4/book1.html) (last access: 2012), 2012. 4453

Zhang, Z. S., Nisancioglu, K., Bentsen, M., Tjiputra, J., Bethke, I., Yan, Q., Risebrobakken, B., Andersson, C., and Jansen, E.: Pre-industrial and mid-Pliocene simulations with NorESM-L, *Geosci. Model Dev.*, 5, 523–533, doi:10.5194/gmd-5-523-2012, 2012. 4453

5

10

## Role insolation and greenhouse gases in timing peak warmth

P. M. Langebroek and  
K. H. Nisancioglu

**Table 1.** Scheme of orbital and greenhouse gas forcing applied in the PI and LIG simulations. Values follow PMIP3 pre-industrial and last interglacial experimental design. Suffix Gpi refers to Greenhouse gas levels (G) at pre-industrial (pi) levels.

Exp. name	Orbital parameters			Greenhouse gas concentrations		
	Ecc	Obl [°]	Peri-180 [°]	CO <sub>2</sub> [ppm]	CH <sub>4</sub> [ppb]	N <sub>2</sub> O [ppb]
PI	0.0167	23.45	102.0	280	760	270
115 ka_Gpi	0.0414	22.41	110.9	280	760	270
120 ka_Gpi	0.0411	23.01	28.0	280	760	270
125 ka_Gpi	0.0400	23.80	307.1	280	760	270
125 ka	0.0400	23.80	307.1	276	640	263
130 ka_Gpi	0.0382	24.24	228.3	280	760	270
130 ka	0.0382	24.24	228.3	257	512	239

[Title Page](#)
[Abstract](#)
[Introduction](#)
[Conclusions](#)
[References](#)
[Tables](#)
[Figures](#)
[Back](#)
[Close](#)
[Full Screen / Esc](#)
[Printer-friendly Version](#)
[Interactive Discussion](#)

## Role insolation and greenhouse gases in timing peak warmth

P. M. Langebroek and  
K. H. Nisancioglu

[Title Page](#)

[Abstract](#)

[Introduction](#)

[Conclusions](#)

[References](#)

[Tables](#)

[Figures](#)



[Back](#)

[Close](#)

[Full Screen / Esc](#)

[Printer-friendly Version](#)

[Interactive Discussion](#)

**Table 2.** Sediment cores considered in this study.

Ocean	Core	Latitude	Longitude	Water depth	Reference(s)
Norwegian Sea	MD95-2010	66.68° N	4.57° E	1226 m	Risebrobakken et al. (2005, 2006)
North Atlantic	ODP 980	55.49° N	14.70° W	2168 m	McManus et al. (1999); Oppo et al. (2006)
Labrador Sea	EW9302-JPC2	48.80° N	45.09° W	1251 m	Rasmussen et al. (2003)
North Atlantic	CH69-K09	41.76° N	47.35° W	4100 m	Cortijo et al. (1999); Labeyrie et al. (1999)

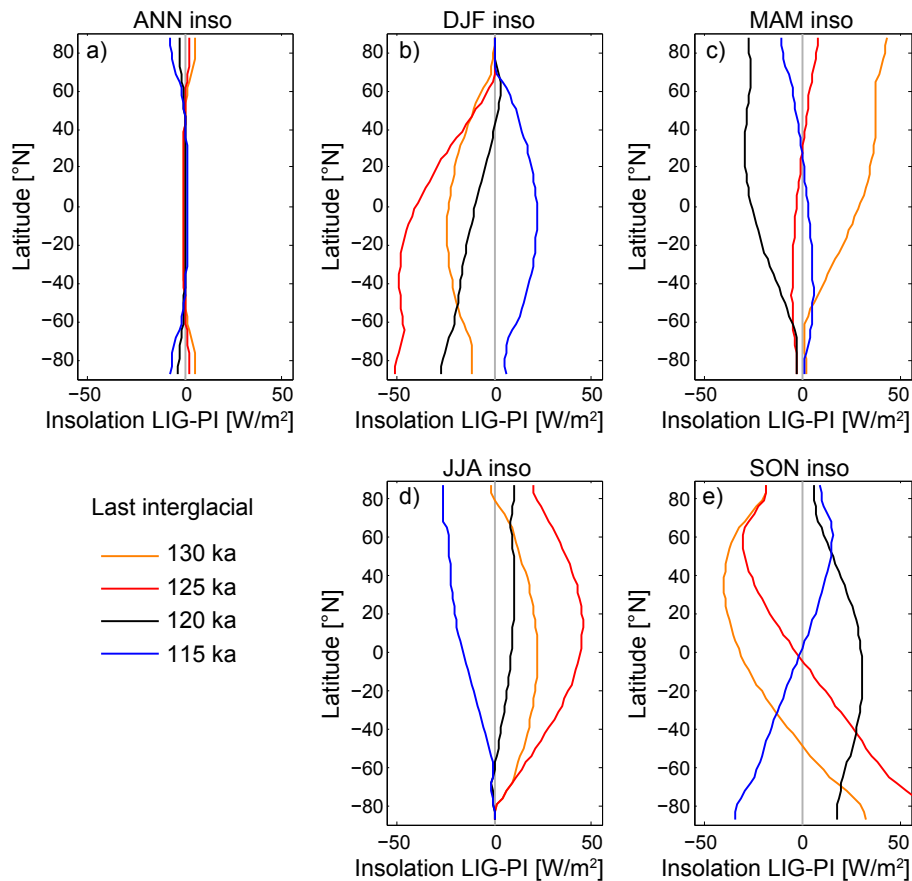


**Fig. 1.** Zonal mean insolation anomalies for the last interglacial (115 ka, 120 ka, 125 ka and 130 ka). **(a)** annual mean; **(b)** winter (DJF) mean; **(c)** spring (MAM) mean; **(d)** summer (JJA) mean; and **(e)** autumn (SON) mean.

## Role insolation and greenhouse gases in timing peak warmth

P. M. Langebroek and  
K. H. Nisancioglu

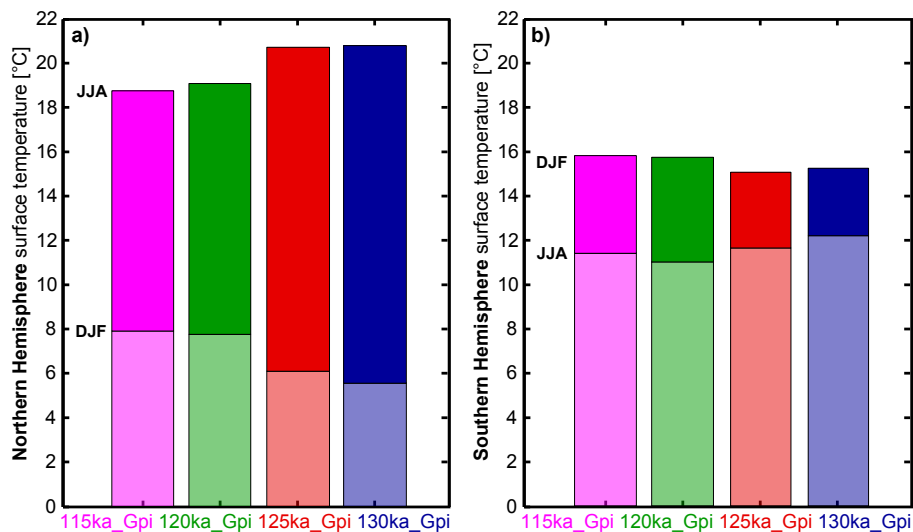


**Fig. 2.** Last interglacial hemispheric mean surface temperatures. **(a)** Northern Hemisphere; and **(b)** Southern Hemisphere. JJA refers to June, July and August, and DJF to December, January and February.

[Title Page](#)
[Abstract](#)
[Introduction](#)
[Conclusions](#)
[References](#)
[Tables](#)
[Figures](#)
[Back](#)
[Close](#)
[Full Screen / Esc](#)
[Printer-friendly Version](#)
[Interactive Discussion](#)

## Role insolation and greenhouse gases in timing peak warmth

P. M. Langebroek and  
K. H. Nisancioglu

Title Page

Abstract

Introduction

Conclusions

References

Tables

Figures



Back

Close

Full Screen / Esc

Printer-friendly Version

Interactive Discussion

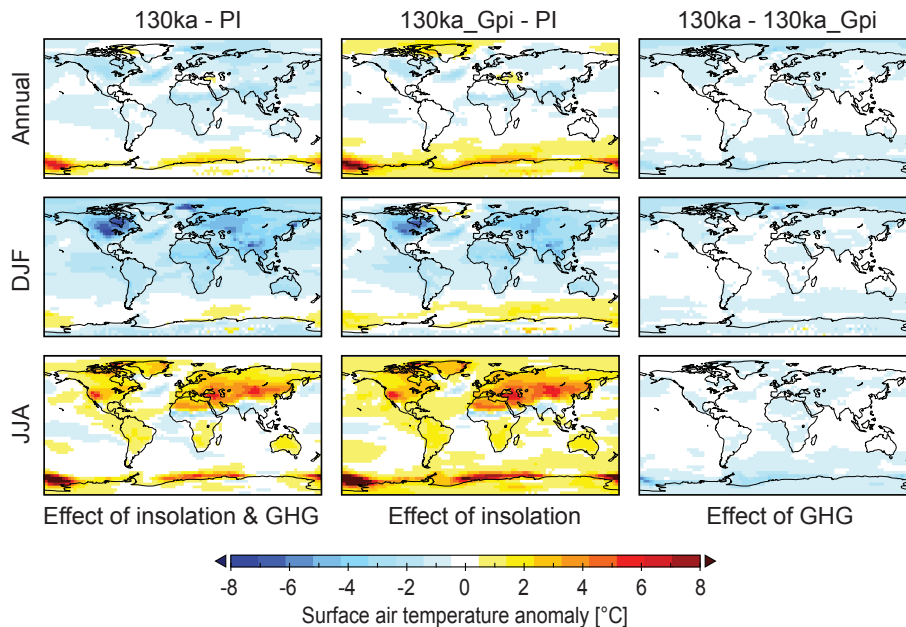


**Fig. 3.** Surface air temperatures difference between 130 ka and pre-industrial. Left column shows run 130 ka (insolation and greenhouse gas forcing for 130 ka), middle column indicates run 130 ka\_Gpi (130 ka insolation and present-day greenhouse gas forcing), right column shows the difference between the first two columns. Upper row shows annual, middle row shows winter (DJF) and bottom row shows summer (JJA) mean temperatures.

## Role insolation and greenhouse gases in timing peak warmth

P. M. Langebroek and  
K. H. Nisancioglu

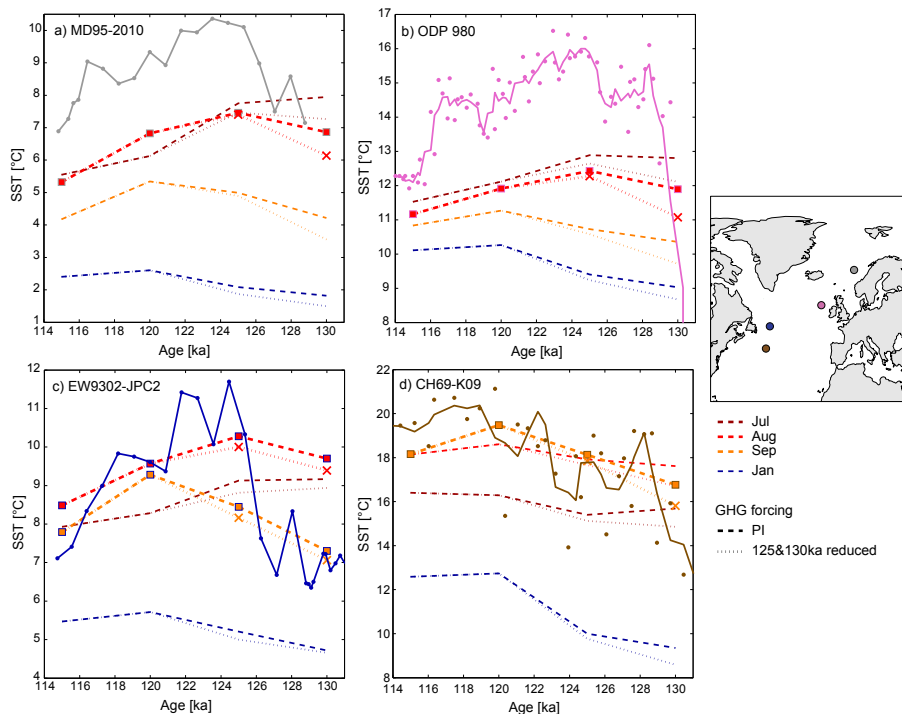


**Fig. 4.** Proxy (solid lines) and modelled (dashed and dotted lines) sea-surface temperatures (SST) for the four core locations. **(a)** Norwegian Sea core MD95-2010; **(b)** North Atlantic core ODP 980; **(c)** Labrador Sea core EW9302-JPC2; and **(d)** North Atlantic core CH69-K09. The dashed lines indicate the modelled last interglacial SST evolution if greenhouse gas forcing was at the constant level of the pre-industrial. The dotted lines show the lower temperatures due to reduced greenhouse gas forcing at 125 ka and 130 ka. The boxes and crosses indicated the modelled SSTs of the month(s) that fits the data best.

## Role insolation and greenhouse gases in timing peak warmth

P. M. Langebroek and  
K. H. Nisancioglu

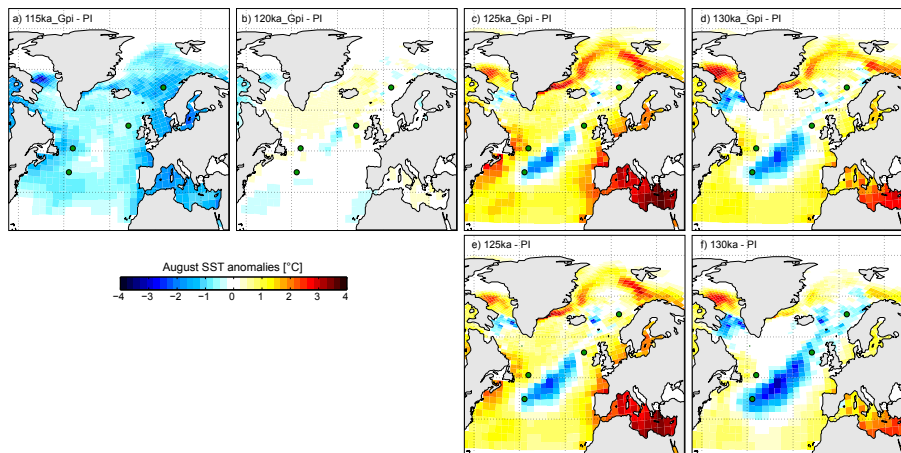


**Fig. 5.** Modelled August sea-surface temperature (SST) anomaly to pre-industrial (PI). Green dots indicate the core locations used in this study. **(a)** 115ka\_Gpi-PI; **(b)** 120ka\_Gpi-PI; **(c)** 125ka\_Gpi-PI; **(d)** 130ka\_Gpi-PI; **(e)** 125ka-PI; **(f)** 130ka-PI. **(a)–(d)** greenhouse gas forcing is fixed to PI; **(e)**, **(f)** greenhouse gas forcing set to 125 ka and 130 ka, respectively.

Title Page

Abstract

Introduction

Conclusions

References

Tables

Figures

◀

▶

◀

▶

Back

Close

Full Screen / Esc

Printer-friendly Version

Interactive Discussion



## Role insolation and greenhouse gases in timing peak warmth

P. M. Langebroek and  
K. H. Nisancioglu

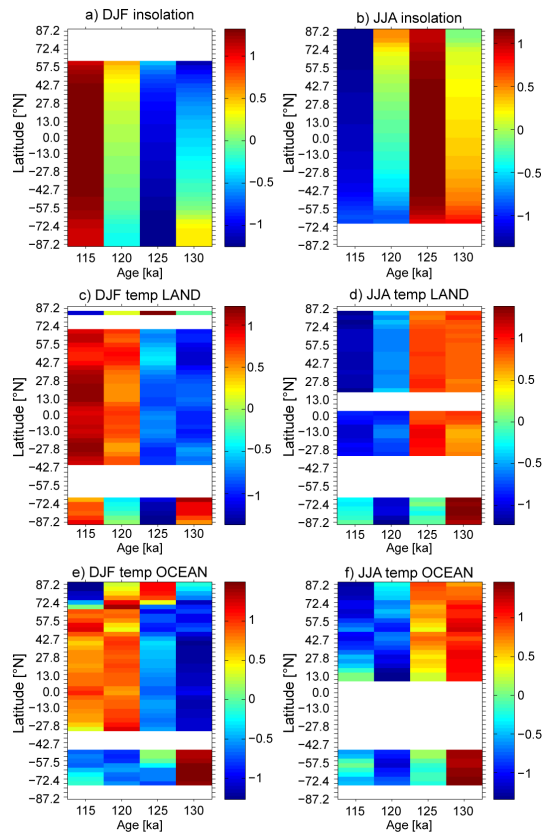


**Fig. 6.** Zonal mean last interglacial insolation and surface air temperature normalized per latitude. **(a)** Winter (DJF) insolation; **(b)** summer (JJA) insolation; **(c)** DJF temperature over land; **(d)** JJA temperature over land; **(e)** DJF temperature over ocean; **(f)** JJA temperature over ocean. Excluded are results for latitudes where the insolation varies less than  $5 \text{ W m}^{-2}$  (Fig. 6a, b) and where the temperature varies less than half of the mean variations ( $0.7^\circ\text{C}$  for Fig. 6c, d and  $0.3^\circ\text{C}$  for Fig. 6e, f).

[Title Page](#)
[Abstract](#)
[Introduction](#)
[Conclusions](#)
[References](#)
[Tables](#)
[Figures](#)

[Back](#)
[Close](#)
[Full Screen / Esc](#)
[Printer-friendly Version](#)
[Interactive Discussion](#)